Characterization of the γδ T-cell compartment during infancy reveals clear differences between the early neonatal period and 2 years of age.

Marieke van der Heiden[1#], Sophia Björkander[1#], Khaleda Rahman Qazi[1], Julia Bittmann[1], Lena Hell[1], Maria C. Jenmalm[2], Giovanna Marchini[3], David Vermijlen[4], Thomas Abrahamsson[2,5], Caroline Nilsson[6,7], Eva Sverremark-Ekström[1]

[#]Contributed equally

[1]*Department of Molecular Biosciences, The Wenner-Gren Institute, Stockholm University, Stockholm, Sweden*

[2]*Department of Clinical and Experimental Medicine, Linköping University, Linköping, Sweden.*

[3]*Department of Women's and Children's Health, Karolinska Institutet, Stockholm, Sweden.*

[4]*Department of Pharmacotherapy and Pharmaceutics and Institute for Medical Immunology, Université Libre de Bruxelles, Bruxelles, Belgium.*

[5]*Department of Clinical and Experimental Medicine and Department of Paediatrics, Linköping University, Linköping, Sweden*

[6]*Sachs' Children and Youth Hospital, Södersjukhuset, Stockholm, Sweden*

[7]*Department of Clinical Science and Education, Södersjukhuset, Karolinska Institutet, Stockholm, Sweden*

Corresponding author: Eva Sverremark-Ekström, eva.sverremark@su.se, Department of Molecular Biosciences, The Wenner-Gren Institute, Stockholm University, 106 91 Stockholm, Sweden.

Running title: γδ T-cells during infancy

Keywords

γδ T-cells, childhood immunity, CMV, prematurity, cord blood, neonatal immunity.

ABSTRACT

γδ T-cells are unconventional T-cells that function on the border of innate and adaptive immunity. They are suggested to play important roles in neonatal and infant immunity, although their phenotype and function are not fully characterized in early childhood.

We aimed to investigate γδ T-cells in relation to age, prematurity, and CMV infection. Therefore, we used flow cytometry to characterize the γδ T-cell compartment in cord blood (CB) and peripheral blood cells from 14-day-, 2-year- and 5-year-old children, as well as in peripheral blood samples collected at several time points during the first months of life from extremely premature neonates.

γδ T-cells were phenotypically similar at 2 and 5 years of age, whereas CB was divergent and showed close proximity to γδ T-cells from 14-days-old neonates. Interestingly, 2-year old children and adults showed comparable $V\delta2^+$ γδ T-cell functionality towards both microbial and polyclonal stimulations. Importantly, extreme preterm birth compromised the frequencies of $V\delta1^+$ cells and affected the functionality of $V\delta2^+$ γδ T-cells shortly after birth. In addition, CMV infection associated with terminal differentiation of the $V\delta1^+$ compartment at 2 years of age.

Our results show an adult-like functionality of the γδ T-cell compartment already at 2 years of age. In addition, we demonstrate an altered γδ T-cell phenotype early after birth in extremely premature neonates, something which possibly could contribute to the enhanced risk for infections in this vulnerable group of children.

INTRODUCTION

γδ T-cells are unconventional T-cells, expressing the γδ T-cell receptor (TCR) [1,2]. The activation of γδ T-cells is non major-histocompatibility-complex (MHC) restricted and these cells can also act as antigen presenting cells (APCs), suggesting that γδ T-cells act on the border of innate and adaptive immunity [3,4,5,6]. γδ T-cells represent 0.5 to 10% of the total circulating lymphocyte population in human adults [1,7,8]. These γδ T-cells are suggested to play important roles in neonatal and infant immunity [1,7,9,10].

γδ T-cells can be further divided into several subsets, based on their γ- and δ- chain TCR usage. The most abundant subset in peripheral blood expresses the γ-chain variable region 9 (Vγ9) and δ-chain variable region 2 (Vδ2). These $V\gamma9^{+}V\delta2^{+}$ cells are percieved to develop in early life and to remain relatively stable until old age [9,11,12]. This γδ T-cell subset responds to phosphoantigens, such as (E)-4-hydroxy-3-methyl-but-2enyl pyrophosphate (HMB-PP), derived from both Gram negative and positive bacteria. Consequently, this subset is important in protection against bacterial infections [1,2,3].

Other γδ T-cell subtypes, of which the majority is $V\delta1^{+}$, are associated with mucosal immunity but can also be found in the periphery [2,3,13]. Current knowledge suggests that $V\delta1^{+}$ γδ T-cells develop towards the end of gestation and decrease in frequency towards adulthood [9,14]. Besides absence of consensus on the activating ligands, cytomegalovirus (CMV) infection has shown to influence this subtype, both during adulthood as well as *in utero* [11,15,16,17,18,19]. In addition, mucosal $V\delta1^{+}$ γδ T-cells might play a role in regulating IgE-mediated allergies, where they are believed to recognize allergens presented by $CD1^{+}$ dendritic cells [13,20].

Several reports describe γδ T-cells during gestation and adulthood, whereas these cells are not fully characterized during early childhood. However, a recent study analyzed the association between nongenetic factors and a broad range of immune dynamics in early childhood and found that CMV and prematurity associated with an altered γδ T-cell compartment during childhood [21]. But how age and prematurity connect with the γδ T-cell compartment during the first weeks and months of life, also considering differentiation and functionality, is not known. Therefore we investigated the phenotype and function of the $V\delta1^{+}$ and $V\delta2^{+}$ γδ T-cell subsets, using samples from cord blood (CB), and peripheral blood samples of 14-days-old neonates, 2- and 5-year-old children as well as from the first months of life from extremely preterm neonates.

78 The results show that CB γδ T-cells closely mimic the phenotype present during the first weeks
79 of life and that there are clear effects of preterm birth on the neonatal γδ T-cell compartment.
80 We further demonstrate that the γδ T-cell compartment in 2-year-old children is both
81 phenotypically and functionally mature and is clearly influenced by CMV serostatus. Together,
82 our results enhance our understanding of γδ T-cell immunity at young age and potentially of
83 childhood immune protection.

RESULTS

2-year-old children possess a mature γδ T-cell compartment

First, the peripheral γδ T-cell pool was investigated in CBMCs (called CB in figures) and PBMCs derived from 2- and 5-year-old children. The frequencies of γδ T-cells **(Figure 1a)**, Vδ1$^+$ γδ T-cells **(Figure 1b)**, and Vδ2$^+$ γδ T-cells among CD3+ cells **(Figure 1c)** were strikingly similar at 2 and 5 years of age, which was also reflected in an equal Vδ1$^+$ over Vδ2$^+$ ratio (**Figure 1d**). In contrast, besides the near absence of Vδ2$^+$ γδ T-cells in CB **(Figure 1c),** CB possessed elevated frequencies of Vδ1$^-$Vδ2$^-$ cells as compared to blood samples from both the 2- and 5-year-old children **(Figure 1e)**. Moreover, 2- and 5-year-old children showed similar frequencies of Vγ9 expressing cells, both within the total CD3$^+$ compartment, as well as among the Vδ1$^+$ and Vδ2$^+$ γδ T-cell subsets, which clearly deviated in CB **(Figure 1f, g, and h)**.

2- and 5- year-old children possessed a significantly lower frequency of cells expressing the differentiation markers CD27 and CD28 in both the Vδ1$^+$ **(Figure 2a, b, and c)** and Vδ2$^+$ **(Figure 2d, e, and f)** compartments as compared to CB, indicating a clear differentiation of these cells already at 2 years of age. In order to verify whether this differentiation of the Vδ2$^+$ subset was associated with the acquisition of a functional response, we verified the IFNγ production after stimulation with either a microbial (HMB-PP) or a polyclonal (CD3:CD28 beads) activator. The Vδ2$^+$ subset at 2 years of age showed an equal frequency of IFNγ$^+$ cells as adult Vδ2$^+$ cells upon both types of stimulations **(Figure 2g and h)**.

The γδ T-cell population is functionally compromised during the early neonatal period

Based on the notable differences in γδ T-cell subsets between CBMCs and PBMCs from 2-year-old children, we extended our analysis with PBMCs from 14-day-old neonates. The PCA analysis (**Figure 3a**) revealed that the γδ T-cell compartment in 14-day-old neonates (blue) was closely related to that of CB (red). The γδ T-cells from 14-day-old neonates and 2-year-old children (yellow) were clearly separated, which was mostly based on higher frequencies of Vδ2$^+$ γδ T-cells in the 2-year-old children. Importantly, although stimulation with HMB-PP enhanced the percentage of IFNγ$^+$Vδ2$^+$ cells in the 14-day-old neonates, the response was significantly lower compared to that at 2 years of age (**Figure 3b**). Interestingly, TCR-mediated stimulation with CD3:CD28 beads induced a robust IFNγ response in the Vδ2$^+$ γδ T-cells from

14-day-old neonates, a response that was statistically higher compared to the 2-year-old children (**Figure 3c**).

γδ T-cells are significantly affected by prematurity

We next investigated the effect of prematurity on the γδ T-cell composition and functionality shortly after birth. CBMCs and PBMCs (collected 14 days, 28 days, and at a timepoint corresponding to postmenstrual week 36) from premature extremely low gestational age neonates (ELGAN) with extremely low birthweight (ELBW), reffered to as PT (preterm). Premature birth significantly affected the frequencies of $V\delta1^+$ γδ T-cells (**Figure 4a**), whereas the frequencies of $V\delta2^+$ γδ T-cells (**Figure 4b**) and $V\delta1^-V\delta2^-$ γδ T-cells (**Figure 4c**) were similar to the fullterm 14-day-old neonates. Furthermore, the frequency of $V\delta1^+$ γδ T-cells was significantly lower in the PT CB samples (**Figure 4d**), whereas a trend to a higher frequency of $V\delta2^+$ γδ T-cells was observed (**Figure 4e**). The $V\delta1^+$ γδ T-cell phenotype clearly differed between the ELGAN/ELBW neonates at postmenstrual week 36 as compared to the 14-day-old neonates, which was mainly related to a higher expression of CD27 and CD28 (**Figure 4g**). Despite similar frequencies of the $V\delta2^+$ cells in ELGAN/ELBW and 14-day-old neonates, phenotypical differences in the Vδ2 compartment at 14 days after birth were observed (**Figure 4h**). This difference was mostly explained by lower frequencies of $V\delta2^+$ cells that express Vγ9 (**Figure 4i**) and Granzyme B (**Figure 4j**) in the ELGAN/ELBW PT neonates, who converged to the pattern found in the 14-day-old neonates at the later timepoints. Interestingly, HMB-PP and CD3:CD28 bead stimulation induced a comparable frequency of $IFN\gamma^+V\delta2^+$ cells in the ELGAN/ELBW PT neonates at postmenstrual week 36 as compared to the 14-day-old neonates (**Figure 4k and l**).

CMV infection is associated with a terminal differentiation of the $V\delta1^+$ γδ T-cell compartment already at 2 years of age

High variation was observed in the γδ T-cell compartment at 2 years of age, which was possibly related to genetical background and/or microbial exposure. We investigated whether infection with CMV, known to influence $V\delta1^+$ γδ T-cells in adults and fetuses, associated with the γδ T-cell phenotype also at 2 years of age. The children were serotyped and divided as being either CMV- and CMV+, based on the presence of CMV-specific antibodies. The Vδ1

compartment at 2 years of age was increased in frequency **(Figure 5a)** and showed a different phenotype (**Figure 5b**) in CMV infected infants. Specifically, the frequencies of Vδ1 cells with a terminally differentiated phenotype; $CD27^{-}CD28^{-}$ (**Figure 5c**), $CD27^{-}CD45RA^{+}$ (**Figure 5d**), $CD57^{+}$ (**Figure 5e**), Granzyme B^{+} (**Figure 5f**), and $CD16^{+}$ (**Figure 5g**) were significantly enhanced in CMV infected children. In contrast, the overall Vδ2 compartment did not diverge between CMV- and CMV+ children (**supplementary figure 3**).

DISCUSSION

Within this study, we demonstrate that 2- and 5-year-old children possess a mature γδ T-cell phenotype, while the γδ T-cell compartment in early post-neonatal life (14 days after birth) is similar to CB. This maturity at 2 years of age is supported by comparable functional responses of the Vδ2$^+$ compartment as in adults towards both a polyclonal (CD3:CD28 beads) and bacterial (HMB-PP) stimulation, while at 14 days after birth this functional response appears to be more restricted. Importantly, we show that extreme preterm birth clearly affects the γδ T-cell phenotype directly after birth, as γδ T-cells collected 14 days after birth from preterm neonates and fullterm neonates display clear phenotypical differences. Finally, we show that early-life CMV infection associates with a distinct Vδ1$^+$ γδ T-cell phenotype at 2 years of age.

Although numerous studies investigate γδ T-cells during adulthood as well as during gestation, little is known about γδ T-cells in early childhood. We show that Vδ2$^+$ γδ T-cells from 2-year-old children and adults are functionally comparable, suggesting mature responses of the Vδ2$^+$ compartment towards bacterial infections at 2 years of age [1,2,3], which is in agreement with others [14]. Interestingly, Vδ2$^+$ cells were recently found resistant towards senescence at old age, suggesting a stable phenotype of these cells once the mature state is reached [11]. On the contrary, Vδ2$^+$ cells are present at very low numbers at birth, a finding that is supported by others [1,14,22,23]. We were able to show that CB samples do closely relate to peripheral samples derived 14 days after birth, indicating that CB is a representative sample when studying early life γδ T-cells. This finding could be γδ T-cell specific, based on the recent report on CB not mirroring neonatal immunity for other immune cells [24]. Nevertheless, a small enhancement of the Vδ2$^+$ γδ T-cell frequency as well as an increased frequency of these cells expressing the Vγ9 chain is observed already 14 days after birth, suggesting a quick start of maturation due to microbial exposure [9,12,14]. These Vδ2$^+$ γδ T-cells at 14 days after birth show a developed capacity to produce IFNγ after a TCR-mediated stimulation, while the response towards HMB-PP is more restricted, possibly indicating an immature response towards bacteria at this age.

Preterm birth clearly affects the γδ T-cell phenotype 14 days after birth and possibly suggests that these cells mature towards the end of full term gestation. This immature Vδ2$^+$ phenotype in ELGAN/ELBW neonates might contribute to the higher bacterial infection burden in these

vulnerable neonates [25] and align with earlier findings that immune cell immaturity is linked to prematurity [26,27]. Subsequently, it is of interest to investigate these Vδ2$^+$ γδ T-cells in a longitudinal manner in a larger cohort of preterm neonates. We demonstrate reduced frequencies of Vδ1$^+$ γδ T-cells after extreme preterm birth, both shortly (14 days) after birth as well as at the timepoint equal to postmenstrual week 36. Notwithstanding, the Vδ1$^+$ frequency tend to increase over time in the preterm neonates, indicating post-gestational maturation of this compartment. These results are in agreement with findings of *Vermijlen et al.*[9], showing sharp increases of Vδ1$^+$ cells towards the end of full term gestation, whereas frequencies were low in gestational week 20-30, the gestational age window of our extreme preterm neonates.

Interestingly, CB samples and samples from 14-day-old neonatals possess relatively high frequencies of Vδ1$^-$Vδ2$^-$ γδ T-cells as compared to all other age groups. These cells might be classified as Vδ3$^+$ or Vδ5$^+$ and frequencies of these cells are known to decline with increasing age, which might be due to homing to mucosal sites [9,23].

Finally, our results indicate that skewing of a large part of the Vδ1$^+$ compartment towards a terminal differentiated, including high cytotoxic potential, phenotype is associated with CMV infection already at 2 years of age, which is similar to what has been reported for γδ T-cells in adults [11,17,28] and older children [29]. Our results indicate that CMV infection in children affects the γδ T-cells in a similar manner as to what is known about αβ T-cells [30,31] and indicate strong anti-viral activity of γδ T-cells already at the age of 2 years. Unfortunately, we are not able to determine functional CMV specific responses, since the ligands of CMV responsive Vδ1$^+$ cells are unknown stress factors secreted by CMV infected cells and consequently hard to mimic *in vitro* [15,18,28]. In addition, our study is not powered to determine effects of CMV infection in the (preterm) neonates, which would be of interest regarding results of *Vermijlen et al*., showing clear effects of *in utero* CMV infection on the fetal Vδ1$^+$ γδ T-cell composition [32]. Moreover, it would be valuable to determine the associations of Epstein-Barr virus (EBV), another potent herpesvirus, with the Vδ1$^+$ γδ T-cell phenotype [33,34]. Moreover, future work could study CMV mediated effects on Vδ1$^+$ γδ T-cells in relation to clinical outcomes, such as infection burden and allergy development during early childhood [13,20].

In conclusion, we provide unique insights in the γδ T-cell phenotype and function at several timepoints during early childhood. The γδ T-cell compartment of preterm infants is clearly affected 14 days after birth but becomes rapidly functional within a few months. Moreover, the γδ T-cell compartment shows maturity at 2 years of age, including comparable functionality to the Vδ2$^+$ γδ T-cells as in adults, both in functional responses of the Vδ2$^+$ subtype, as well as the effects of CMV infection on the Vδ1$^+$ subtype. These results contribute to a better understanding of γδ T-cell immunity in early life, which is important for our knowledge on immune function and protection against infections at young age.

METHODS

Cohort material

Cord blood mononuclear cells (CBMCs) and peripheral blood mononuclear cells (PBMCs) from different cohorts were combined in this study.

CBMCs (n=19) (called CB in figures) and PBMCs from 2-year-old (n=52) and 5-year-old (n=16) children were randomly chosen from a prospective birth cohort, as described elsewhere [35]. All children were born at term between 1997 and 2000 in the Stockholm area and had birth weights within the normal range. This cohort was recruited at the Sachs' Children's Hospital and the study was approved by the Human Ethics Committee at Huddinge University Hospital, Stockholm (Dnr. 75/97, 33/02). All parent provided informed consent.

Moreover, CBMCs and PBMCs were used from a prospective, randomized-controlled, multi-center trial; PROPEL (Prophylactic Probiotics to Extremely Low Birth Weight Premature Infants). The study was executed in 10 neonatal units between 2012 and 2015 in the region of Stockholm and Linköping and is described in detail elsewhere [36]. The study was approved by the Ethics Committee for Human Research in Linköping (Dnr 2012/28-31, Dnr 2012/433-32). In short, infants were eligible for participation between gestational week 23+0 and 27+6 and with a birthweight less than 1000g. CBMCs (n=4) and PBMCs from several timepoints after birth were used: 14 days (14d) (n=4), 28 days (28d) (n=3), and at post menstrual week 36 (w36) (n=10) (all reffered to as preterm (PT)). In addition, PBMCs from full term born children were collected 14 days after birth (n=10) (reffered to as 14-day-old neonates).

Adult PBMCs (n=10) were collected from healthy volunteers, which was approved by the Regional Ethics Committee at Karolinska Institute, Stockholm, Sweden (Dnr. 04-106/1 2014/2052-32). For all human material, the use of the samples was performed in accordance with GDPR and the correct explicit authorizations were obtained.

Cord and peripheral blood mononuclear cell isolation

Cord and peripheral blood was collected in collection tubes containing heparin (BD Biosciences Pharmingen, San Jose, California). CBMCs and PBMCs were isolated with gradient separation using Ficoll-Hypaque (GE Healthcare Bio-sciences AB, Uppsala, Sweden). The cells were washed using RPMI-1640 (GE Healthcare Life Sciences, Hyclone laboratories, Utah, USA) and thereafter frozen in freezing media containing 40% RPMI-1640, 50% FCS and 10%

dimethyl sulphoxide (DMSO) (all Sigma Aldrich, St Louis, Missouri, USA) and stored in liquid nitrogen until further use.

Processing and In vitro stimulation of PBMCs

Frozen CBMCs and PBMCs were thawed and washed with RPMI-1640 supplemented with 20 mM HEPES (GE Healthcare Life Sciences). The cells were counted and viability was assessed with Trypan Blue staining, only cells with sufficient viability were used for the functional assays. Subsequently, the cells were resuspended in a concentration of 10^6 cells/mL in cell culture medium, consisting of RPMI-1640 supplemented with 20 mM HEPES, 100 U mL^{-1} penicillin, 100 ug mL^{-1} streptomycin, 2 mM L-glutamate (2 mM) (all GE Healthcare Life Sciences), and 10% heat-inactivated FCS (Sigma Aldrich). The cells were either rested for a minimum of one hour before basal phenotypic staining, or stimulated for 24 hours with 40 ng mL^{-1} (E)-4-hydroxy-3-methyl-but-2-enyl pyrophosphate (HMB-PP) (Sigma Aldrich) or Dynabeads™ Human T-activator CD3:CD28 (Thermo Fisher Scientific, Waltham, Massachusetts, USA) at a 2:1 cell:bead ratio at 37°C and 5% CO_2 in a flat-bottomed 48 well plate (Costar, Cambridge, UK). Brefeldin A (BD Biosciences, San Jose, CA, USA) was added during the last 4 hours of incubation.

Flow cytometric analysis

The cells were washed with PBS and stained with live/dead FVS780 (BD Biosciences) in PBS, followed by a blocking step with 10% human serum in FACS wash buffer containing PBS, 0.1% BSA (Roche diagnostics GMBH, Mannheim, Germany), and 2mM EDTA (Invitrogen, Grand Island, NY). Subsequently, the cells were surface stained with the following antibodies in FACS wash buffer: CD3-BV510 (Clone: UCHT-1), Vδ2-APC (Clone: B6) (both Biolegend, San Diego, CA), and Vδ1-PE-Cy7 (Beckman Coulter, Brea, CA) together with several combinations of the following antibodies: Panγδ TCR-FITC (Clone: Immu510), Vγ9-FITC (both Beckman Coulter), CD27-PE (Clone: M-T271), CD45RA-FITC (Clone: H1100), CD158b/j-PE (Clone: DX27) (all Biolegend), CD28-BV421 (Clone: CD28.2), CD57-FITC (Clone: NK-1) or CD16-BV421 (Clone: 3G8) (BD Biosciences). After surface staining, cells were either washed and fixed with 4% PFA before analysis or treated with the Intracellular staining fixation kit (Biolegend) according to the manufacturers' instructions. The cells were intracellularly blocked with 10% human serum and stained with Perforin-FITC (Clone: B-D48) (Biolegend) and GranzymeB-V450 (Clone: GB-

11) (BD Biosciences) in intracellular staining perm/wash buffer (Biolegend). HMB-PP and CD3:CD28 beads stimulated cells were intracellularly stained with IFNγ-PerCP Cy5.5 (Clone: B27) (BD Biosciences). The data was acquired with a Facs Verse in combination with the Facs Suite software (BD Biosciences). Fluorescence-minus-one (FMO) and isotype controls were used for gating. Example gating strategies are provided in **supplementary figure 1 and 2**.

Detection of CMV infection status

CMV infection status was based on the presence of CMV IgG antibodies in plasma samples. These IgG antibodies were determined with an in-house CMV-IgG ELISA described elsewhere [37].

Statistical analysis

All data was checked for normality distribution before statistical analysis. In all graphs, the median with 95% CI is displayed. Three or more different age groups were compared with the Kruskal-Wallis test followed by the Dunn's multiple comparisons test. The unstimulated (US) and HMB-PP or CD3:CD28 beads stimulated samples were compared with the Wilcoxon matched-pairs signed rank test. Two different age groups or the CMV- and CMV+ groups were compared with the Mann-Whitney *U* test. A *P*-value < 0.05 was considered significant. Significances are indicated with: **P* < 0.05, ***P* < 0.01, ****P* < 0.001, *****P* < 0.0001. For these analysis, GraphPad Prism V7 was used.

The principal components analyses (PCA) were performed using SPSS V25 and GraphPad Prism V7. Different combinations of cell subset frequencies were used in this analysis, as mentioned in the figure legends. The data was reduced into two principal components, of which the amount of variance in the data that is explained by the component is mentioned as a percentage on the axes. Also, the total variance in the data that is explained by the two principal components combined is indicated in the graphs. The validity of the PCA was checked with the Kaiser-Meyer-Olkin Measure of Sampling Adequacy and the Bartlett's Test of Sphericity. Subset frequencies that explained most variation, including the direction of the relation, were indicated with arrows in the plots. Different age groups are indicated with different colors, as explained in the figure legends.

AUTHOR CONTRIBUTIONS

SB, DV and ESE conceptualized the study. CN, GM and TA included study participants and performed all clinical examinations. SB, MCJ and KRQ collected the material and prepared all cells. MvdH and SB designed the experiments. MvdH, SB, JB and LH performed the experiments and analyzed the data in collaboration with all co-authors. MvdH, SB, and ESE wrote the manuscript. All authors critically revised the manuscript.

ACKNOWLEDGEMENTS

We thank all the participants and their parents for their cooperation and the nurses involved in blood drawings.

This works was supported by: The Swedish Research Council (2016-01715_3), the Torsten Söderberg Foundation, the Cancer and Allergy Foundation, the Swedish Asthma and Allergy Association's Research Foundation, the Hesselman Foundation, the Golden Jubilee Memorial Foundation, the Crownprincess Lovisa/Axel Tielman Foundations, the Engkvist Foundations, the Swedish Heart-Lung Foundation, and the Hedlund Foundation.

CONFLICT OF INTEREST

All authors declare no conflict of interest.

REFERENCES

1. Vermijlen D, Prinz I. Ontogeny of innate T lymphocytes - some innate lymphocytes are more innate than others. *Front Immunol.* 2014; **5:** 1–12.
2. Gao Y, Williams AP. Role of innate T cells in anti-bacterial immunity. *Front Immunol.* 2015; **6:** 1-8.
3. Tyler CJ, Doherty DG, Moser B, *et al*. Human Vγ9/Vδ2 T cells: Innate adaptors of the immune system. *Cell Immunol.* 2015; **1:** 10–21.
4. Bonneville M, O'Brien RL, Born WK. γ δ T cell effector functions: A blend of innate programming and acquired plasticity. *Nat Rev Immunol.* 2010; **10:** 467–478.
5. Lawand M, Déchanet-Merville J, Dieu-Nosjean MC. Key features of gamma-delta T-cell subsets in human diseases and their immunotherapeutic implications. *Front Immunol.* 2017; **8:** 1-9
6. Parker CM, Groh V, Band H, *et al.* Evidence for extrathymic changes in the T cell receptor gamma/delta repertoire. *J Exp Med.* 2004; **171:** 1597–1612.
7. Gibbons DL, Haque SFY, Silberzahn T, *et al.* Neonates harbour highly active γδ T cells with selective impairments in preterm infants. *Eur J Immunol.* 2009; **39:** 1794–1806.
8. Paul S, Shilpi, Lal G. Role of gamma-delta (γδ) T cells in autoimmunity . *J Leukoc Biol.* 2014; **97:** 259–271.
9. Dimova T, Brouwer M, Gosselin F, *et al.* Effector Vγ9Vδ2 T cells dominate the human fetal γδ T-cell repertoire. *Proc Natl Acad Sci.* 2015; **112:** E556–E565.
10. Godfrey DI, Uldrich AP, Mccluskey J, *et al.* The burgeoning family of unconventional T cells. *Nat Immunol.* 2015; **16:** 1114–1124.
11. Xu W, Monaco G, Wong EH, *et al.* Mapping of γ/δ T cells reveals Vδ2+ T cells resistance to senescence. *EBioMedicine.* 2019; **39:** 44–58.
12. Willcox CR, Davey MS, Willcox BE. Development and selection of the human Vγ9Vδ2+T-Cell Repertoire. *Front Immunol.* 2018; **9:** 1–7.
13. McCarthy NE, Eberl M. Human γδ T-cell control of mucosal immunity and inflammation. *Front Immunol.* 2018; **9:** 1-8.
14. De Rosa SC, Andrus JP, Perfetto SP, *et al.* Ontogeny of T Cells in Humans. *J Immunol.* 2004; **172:** 1637–1645.
15. Vermijlen D, Gatti D, Kouzeli A, *et al.* γδ T cell responses: How many ligands will it take

till we know? *Semin Cell Dev Biol.* 2018; **84:** 75–86.

16. Willcox BE, Willcox CR. γδ TCR ligands: the quest to solve a 500-million-year-old mystery. *Nat Immunol.* 2019; **20:** 121–128.

17. Kallemeijn MJ, Boots AMH, Van Der Klift MY, *et al.* Ageing and latent CMV infection impact on maturation, differentiation and exhaustion profiles of T-cell receptor gammadelta T-cells. *Sci Rep.* 2017; **7:** 1–14.

18. Willcox CR, Pitard V, Netzer S, *et al.* Cytomegalovirus and tumor stress surveillance by binding of a human γδ T cell antigen receptor to endothelial protein C receptor. *Nat Immunol.* 2012; **13:** 872–879.

19. Pitard V, Roumanes D, Lafarge X, *et al.* Long-term expansion of effector/memory V 2- T cells is a specific blood signature of CMV infection. *Blood.* 2008; **112:** 1317–1324.

20. Huang Y, Yang Z, McGowan J, *et al.* Regulation of IgE Responses by γδ T Cells. *Curr Allergy Asthma Rep.* 2015; **15:** 1-8.

21. van den Heuvel D, Jansen MAE, Nasserinejad K, *et al.* Effects of nongenetic factors on immune cell dynamics in early childhood: The Generation R Study. *J Allergy Clin Immunol.* 2017; **139:** 1923-1934.e17.

22. Morita CT, Parker CM, Brenner MB, *et al.* TCR usage and functional capabilities of human gamma delta T cells at birth. *J Immunol.* 1994; **153:** 3979–3988.

23. Kalyan S, Kabelitz D. Defining the nature of human γδ T cells: A biographical sketch of the highly empathetic. *Cell Mol Immunol.* 2013; **10:** 21–29.

24. Olin A, Henckel E, Chen Y, *et al.* Stereotypic Immune System Development in Newborn Children. *Cell.* 2018; **174:** 1277-1292.e14.

25. Stoll BJ, Hansen N, Fanaroff AA, *et al.* Late-Onset Sepsis in Very Low Birth Weight Neonates: The Experience of the NICHD Neonatal Research Network. *Pediatrics.* 2002; **110:** 285–291.

26. Scheible KM, Emo J, Laniewski N, *et al.* T cell developmental arrest in former premature infants increases risk of respiratory morbidity later in infancy. *JCI Insight.* 2018; **3:** 1–17.

27. Strunk T, Currie A, Richmond P, *et al.* Innate immunity in human newborn infants: prematurity means more than immaturity. *J Matern Neonatal Med.* 2011; **24:** 25–31.

28. Khairallah C, Déchanet-Merville J, Capone M. γδ T cell-mediated immunity to cytomegalovirus infection. *Front Immunol.* 2017; **8:** 1-13.

29. Jansen MAE, van den Heuvel D, Jaddoe VWV, *et al.* Abnormalities in CD57 + cytotoxic T cells and Vδ1 + γδT cells in subclinical celiac disease in childhood are affected by cytomegalovirus. The Generation R Study. *Clin Immunol.* 2017; **183:** 233–239.
30. Sohlberg E, Saghafian-Hedengren S, Rasul E, *et al.* Cytomegalovirus-Seropositive Children Show Inhibition of In Vitro EBV Infection That Is Associated with $CD8^{+}CD57^{+}$ T Cell Enrichment and IFN-. *J Immunol.* 2013; **191:** 5669–5676.
31. Van Den Heuvel D, Jansen MAE, Dik WA, *et al.* Cytomegalovirus- and epstein-barr virus-induced T-cell expansions in young children do not impair naive T-cell populations or vaccination responses: The Generation R study. *J Infect Dis.* 2016; **213:** 233–242.
32. Vermijlen D, Brouwer M, Donner C, *et al.* Human cytomegalovirus elicits fetal γδ T cell responses in utero. *J Exp Med.* 2010; **207:** 807–821.
33. Kotsiopriftis M, Tanner JE, Alfieri C. Heat Shock Protein 90 Expression in Epstein-Barr Virus-Infected B Cells Promotes T-Cell Proliferation In Vitro. *J Virol.* 2005; **79:** 7255–7261.
34. Xiang Z, Liu Y, Zheng J, *et al.* Targeted Activation of Human Vγ9Vδ2-T Cells Controls Epstein-Barr Virus-Induced B Cell Lymphoproliferative Disease. *Cancer Cell.* 2014; **26:** 565–576.
35. Nilsson C, Linde A, Montgomery SM, *et al.* Does early EBV infection protect against IgE sensitization? *J Allergy Clin Immunol.* 2005; **116:** 438–444.
36. Wejryd E, Marchini G, Frimmel V, *et al.* Probiotics promoted head growth in extremely low birthweight infants in a double-blind placebo-controlled trial. *Acta Paediatr Int J Paediatr.* 2019; **108:** 62–69.
37. Grillner L. Screening of blood donors for cytomegalovirus (CMV) antibodies: an evaluation of different tests. *J Virol Methods.* 1987; **17:** 133–139.

Figure legends

Figure 1. The frequency of γδ T-cell subsets in CB and PBMCs from 2- and 5-year-old children.

(a) The frequencies of PanγδTCR$^+$ cells among CD3$^+$ cells in CBMCs (CB) (n=19) and PBMCs from 2-year-old (2y) (n=52) and 5-year-old (5y) (n=16) children. The frequencies of Vδ1$^+$PanγδTCR$^+$ cells among CD3+ cells **(b)**, Vδ2$^+$PanγδTCR$^+$ cells among CD3$^+$ cells **(c)**, the Vδ1$^+$PanγδTCR$^+$/ Vδ2$^+$PanγδTCR$^+$ cell ratio **(d)**, Vδ1$^-$Vδ2$^-$ cells among PanγδTCR$^+$ cells **(e),** Vγ9$^+$ cells among CD3$^+$ cells **(f)**, Vγ9$^+$ cells among Vδ1$^+$ cells **(g)**, and Vγ9$^+$ cells among Vδ2$^+$ cells **(h)** in CB (n=12), and in PBMCs from 2- (n=28) and 5- (n=16) year-old children.

Figure 2. The differentiation and functionality of γδ T-cells in CB and PBMCs from 2- and 5-year-old children.

The frequencies of CD27$^+$ cells among Vδ1$^+$ cells **(a)**, CD28$^+$ cells among Vδ1$^+$ cells **(b)**, and CD27$^-$CD28$^-$ cells among Vδ1$^+$ cells **(c).** The frequencies of CD27$^+$ cells among Vδ2$^+$ cells **(d)**, CD28$^+$ cells among Vδ2$^+$ cells **(e)**, and CD27$^-$CD28$^-$ cells among Vδ2$^+$ cells **(f)** in CB (n=12), and PBMCs from 2-(n=28) and 5-(n=16) year-old children. The frequency of IFNγ$^+$ cells among Vδ2$^+$ cells after 24-hour stimulation with HMB-PP **(g)** or CD3:CD28 beads **(h)** in PBMCs from 2-year-old children (n=13 and n=6 respectively) and adults (n=10 and n=7 respectively).

Figure 3. The γδ T-cell compartment in PBMCs from 14-days-old neonates.

(a) Principal component analysis (PCA) comparing the γδ T-cell phenotype of CB (red)(n=12), 14-day-old neonates (blue)(n=10), and 2-year-old children (yellow)(n=17). The total frequencies of PanγδTCR$^+$ cells among CD3$^+$ cells as well as the frequencies of Vδ2$^+$PanγδTCR$^+$ cells among CD3$^+$ cells, Vδ1$^+$PanγδTCR$^+$ cells among CD3$^+$ cells and Vδ1$^-$ Vδ2$^-$ cells among PanγδTCR$^+$ cells were included in the PCA analysis. The frequency of IFNγ$^+$ cells among Vδ2$^+$ cells after 24-hour stimulation with HMB-PP **(b)** or CD3:CD28 beads **(c)** between the 14-day-old neonates (n=8 and n=5 respectively) and 2-year-old children (n=13 and n=10 respectively).

Figure 4. The γδ T-cell phenotype and function in preterm neonates.

The frequencies of Vδ1$^+$PanγδTCR$^+$ cells among CD3$^+$ cells **(a)**, Vδ2$^+$PanγδTCR$^+$ cells among CD3$^+$ cells **(b)** and Vδ1$^-$Vδ2$^-$ cells among PanγδTCR$^+$ cells **(c)** in 14-day-old full term neonates (14d, n=10) and preterm (PT) neonates at different timepoints after birth (CB (n=4), 14 days (14d) (n=4), 28 days (28d) (n=3), and at post menstrual age week 36 (36w) (n=10)).

The frequencies of Vδ1$^+$PanγδTCR$^+$ cells among CD3$^+$ cells **(d)**, Vδ2$^+$PanγδTCR$^+$ cells among CD3$^+$ cells **(e)**, and Vδ1$^-$Vδ2$^-$ cells among PanγδTCR$^+$ cells **(f)** in CB samples from preterm (CB PT, n=4) and fullterm CB samples (CB, n=12).

(g) PCA analysis comparing the Vδ1 phenotype between the full term 14-day-old neonates (14-day-old, blue) and preterm neonates at postmenstrual week 36 (PT 36 weeks, yellow). The analysis includes the frequencies of CD27$^+$, CD28$^+$, CD161$^+$, GrzB$^+$, perforin$^+$ and Vγ9$^+$ cells among Vδ1$^+$ cells. **(h)** PCA analysis comparing the Vδ2 phenotype between the 14-day-old neonates (blue), and preterm (PT) newborns at 14 days (red), 28 days (green), and postmenstrual week 36 (yellow). The analysis includes the frequencies of CD28$^+$, CD27$^+$, CD27$^-$CD28$^-$, CD161$^+$, GrzB$^+$, and Vγ9$^+$ cells among Vδ2$^+$ cells.

The frequencies of Vγ9$^+$ cells among Vδ2$^+$ cells **(i)**, and Granzyme B (GrzB$^+$) among Vδ2$^+$cells **(j)** between 14-day-old neonates (n=10) and preterm (PT) neonates at different timepoints after birth (14 days (14d) (n=4), 28 days (28d) (n=3), and at post menstrual age week 36 (36w) (n=10)).

The frequency of IFNγ$^+$ cells among Vδ2$^+$ cells after 24-hour stimulation with HMB-PP **(k)** or CD3:CD28 beads **(l)** in the 14-day-old neonates (n=8 and n=5 respectively) and the preterm neonates at postmenstrual week 36 (PT 36 weeks) (n=4 and n=4 respectively).

Figure 5. The Vδ1 phenotype in CMV infected and non-infected 2-year-old children.

(a) The frequency of Vδ1$^+$ cells among CD3$^+$ cells in CMV- (n=17) and CMV+ (n=15) 2-year-old children. **(b)** PCA analysis of the Vδ1 phenotype comparing CB (red)(n=7), CMV negative (CMV-, yellow) (n=12), and CMV infected (CMV+, blue) (n=10) 2-year-old children. The frequencies of CD28$^+$, CD27$^+$, CD161$^+$, CD27$^-$CD28$^-$, CD27$^-$CD45RA$^+$, CD57$^+$, GrzB$^+$, CD16$^+$, perforin$^+$, CD158b$^+$, and CD45RA$^+$ cells among the Vδ1$^+$ cells are included in the analysis.

The frequency of CD27$^-$CD28$^-$ **(c)**, CD27$^-$CD45RA$^+$ **(d)**, CD57$^+$ **(e)**, GrzB$^+$ **(f)**, and CD16$^+$ **(g)** cells among Vδ1$^+$ cells in CMV- (n=17) and CMV+ (n=15) 2-year-old children.

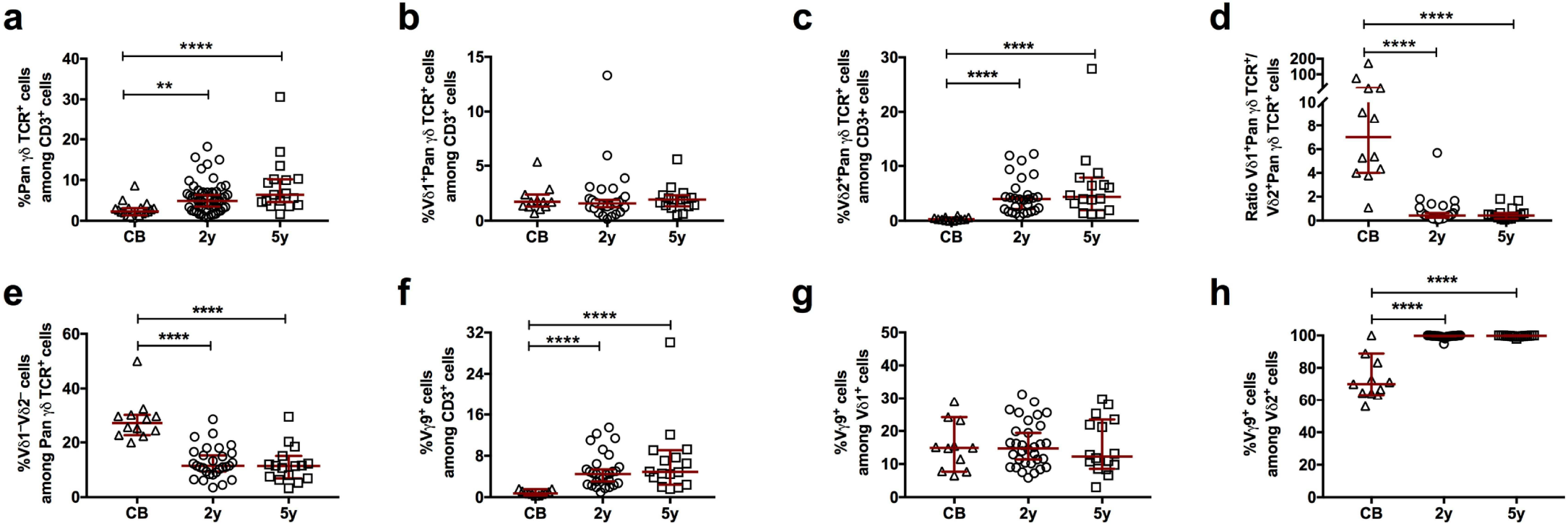
a
%Pan γδ TCR+ cells among CD3+ cells
40
30
20
10
0
****
**
CB
2y
5y
b
%Vδ1+Pan γδ TCR+ cells among CD3+ cells
15
10
5
0
CB
2y
5y
c
%Vδ2+Pan γδ TCR+ cells among CD3+ cells
30
20
10
0
****
****
CB
2y
5y
d
Ratio Vδ1+Pan γδ TCR+/ Vδ2+Pan γδ TCR+ cells
200
100
10
8
6
4
2
0
****
****
CB
2y
5y
e
%Vδ1−Vδ2− cells among Pan γδ TCR+ cells
60
40
20
0
****
****
CB
2y
5y
f
%Vγ9+ cells among CD3+ cells
32
24
16
8
0
****
****
CB
2y
5y
g
%Vγ9+ cells among Vδ1+ cells
50
40
30
20
10
0
CB
2y
5y
h
%Vγ9+ cells among Vδ2+ cells
100
80
60
40
20
0
****
****
CB
2y
5y

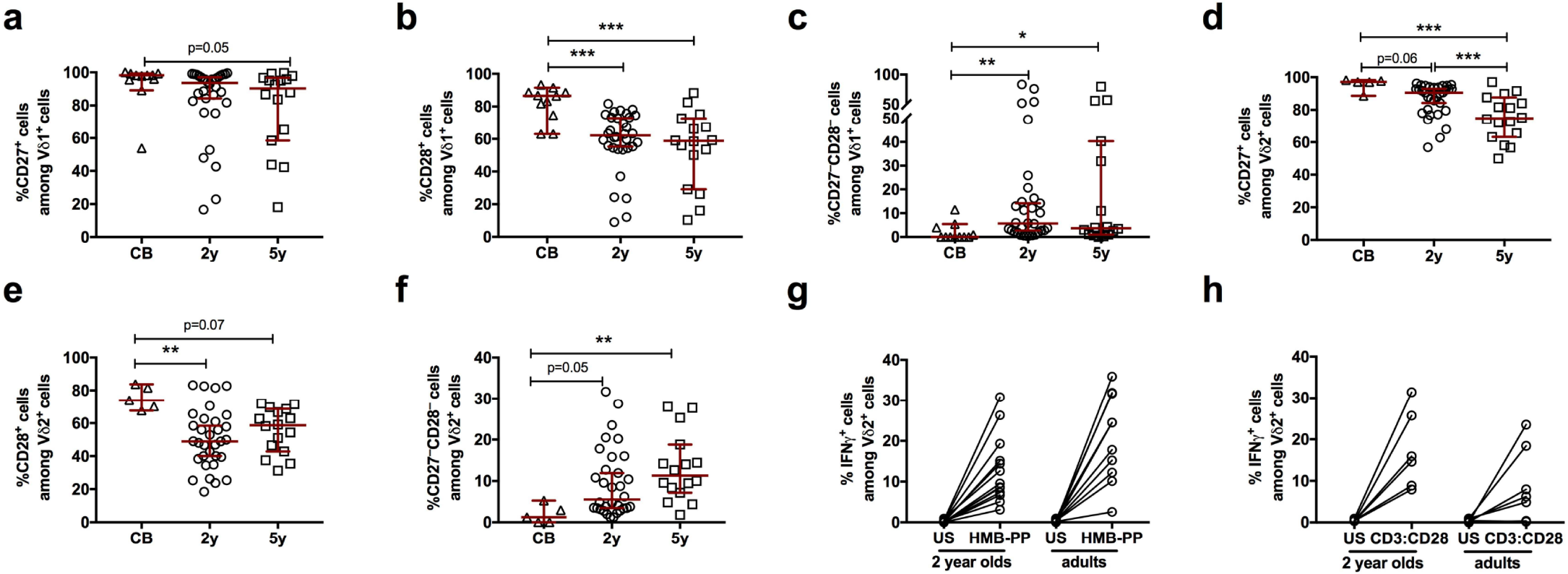
a
p=0.05
%CD27+ cells among Vδ1+ cells
CB
2y
5y
b
***
***
%CD28+ cells among Vδ1+ cells
c
*
**
%CD27−CD28− cells among Vδ1+ cells
d
***
p=0.06
***
%CD27+ cells among Vδ2+ cells
e
p=0.07
**
%CD28+ cells among Vδ2+ cells
f
**
p=0.05
%CD27−CD28− cells among Vδ2+ cells
g
% IFNγ+ cells among Vδ2+ cells
US
HMB-PP
US
HMB-PP
2 year olds
adults
h
% IFNγ+ cells among Vδ2+ cells
US CD3:CD28
US CD3:CD28
2 year olds
adults

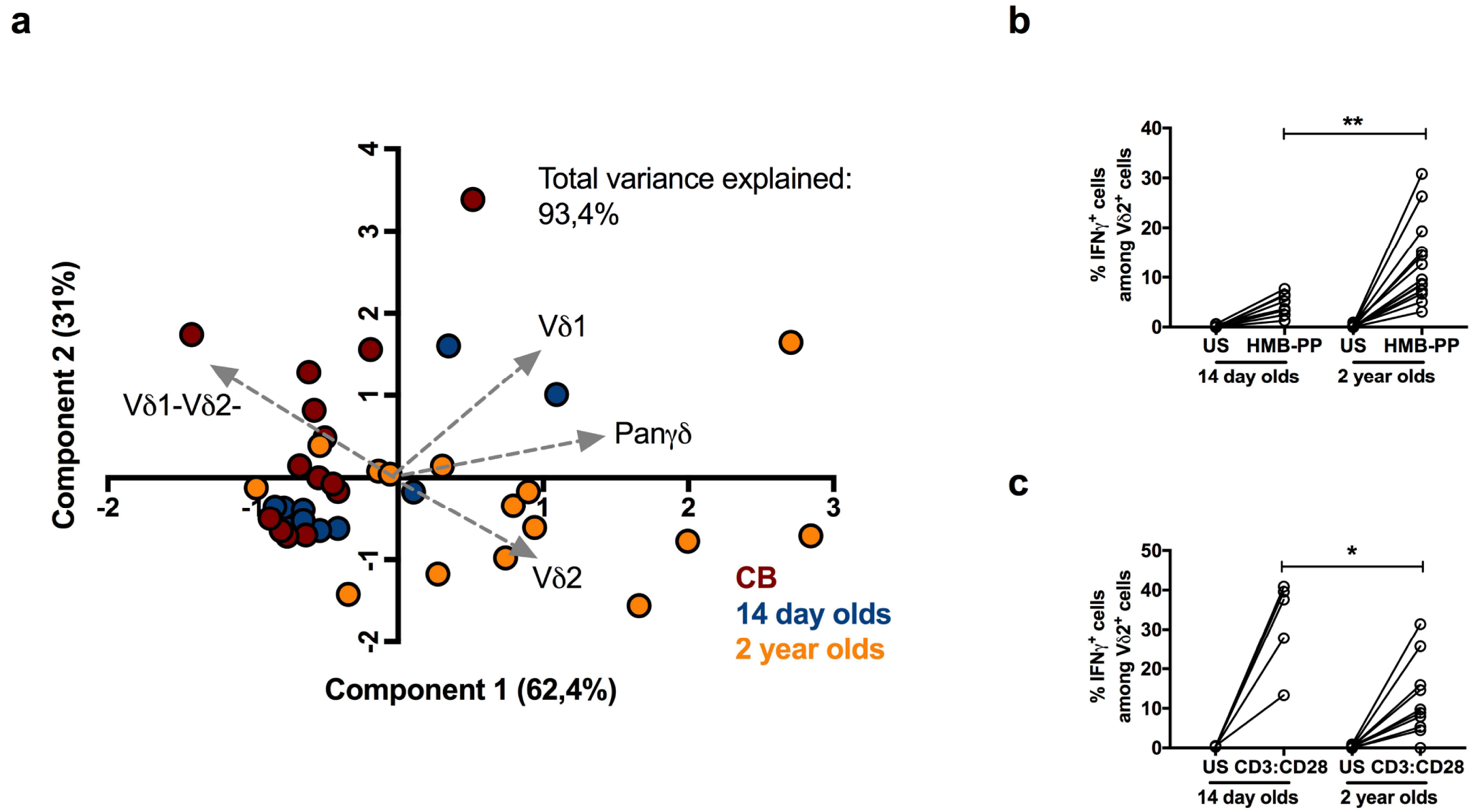
a
Total variance explained:
93,4%
Vδ1
Panγδ
Vδ2
Vδ1-Vδ2-
Component 2 (31%)
Component 1 (62,4%)
CB
14 day olds
2 year olds
b
% IFNγ+ cells among Vδ2+ cells
**
US
HMB-PP
US
HMB-PP
14 day olds
2 year olds
c
% IFNγ+ cells among Vδ2+ cells
*
US CD3:CD28
US CD3:CD28
14 day olds
2 year olds

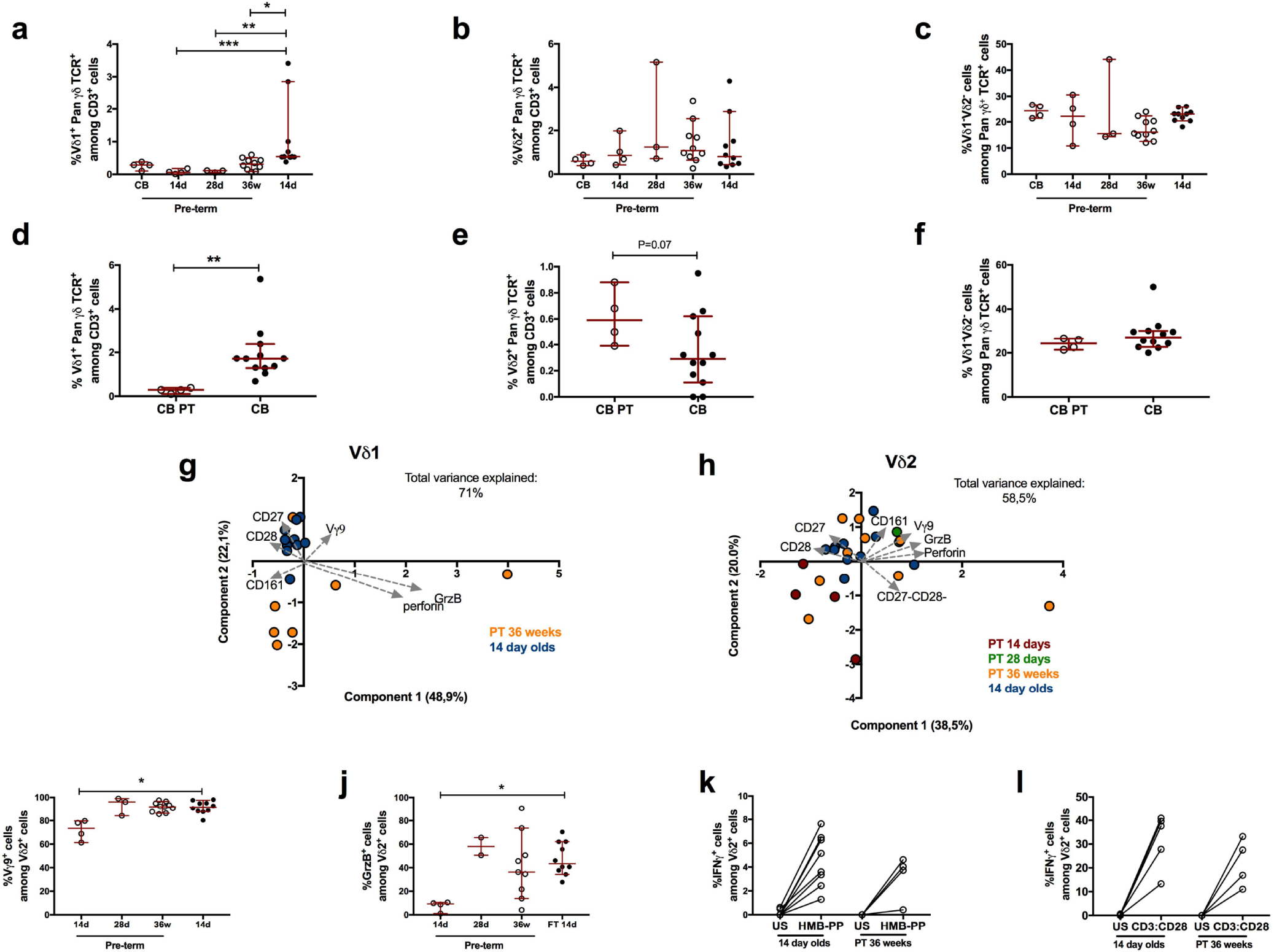
a
%Vδ1+ Pan γδ TCR+ among CD3+ cells
CB
14d
28d
36w
14d
Pre-term
b
%Vδ2+ Pan γδ TCR+ among CD3+ cells
c
%Vδ1-Vδ2- cells among Pan γδ+ TCR+ cells
d
% Vδ1+ Pan γδ TCR+ among CD3+ cells
CB PT
CB
e
P=0.07
% Vδ2+ Pan γδ TCR+ among CD3+ cells
f
% Vδ1-Vδ2- cells among Pan γδ TCR+ cells
g
Vδ1
Total variance explained: 71%
CD27
CD28
CD161
Vγ9
GrzB
perforin
Component 2 (22,1%)
Component 1 (48,9%)
PT 36 weeks
14 day olds
h
Vδ2
Total variance explained: 58,5%
CD27
CD28
CD161
Vγ9
GrzB
Perforin
CD27-CD28-
Component 2 (20.0%)
Component 1 (38,5%)
PT 14 days
PT 28 days
PT 36 weeks
14 day olds
i
%Vγ9+ cells among Vδ2+ cells
14d
28d
36w
14d
Pre-term
j
%GrzB+ cells among Vδ2+ cells
14d
28d
36w
FT 14d
Pre-term
k
%IFNγ+ cells among Vδ2+ cells
US
HMB-PP
US
HMB-PP
14 day olds
PT 36 weeks
l
%IFNγ+ cells among Vδ2+ cells
US CD3:CD28
US CD3:CD28
14 day olds
PT 36 weeks

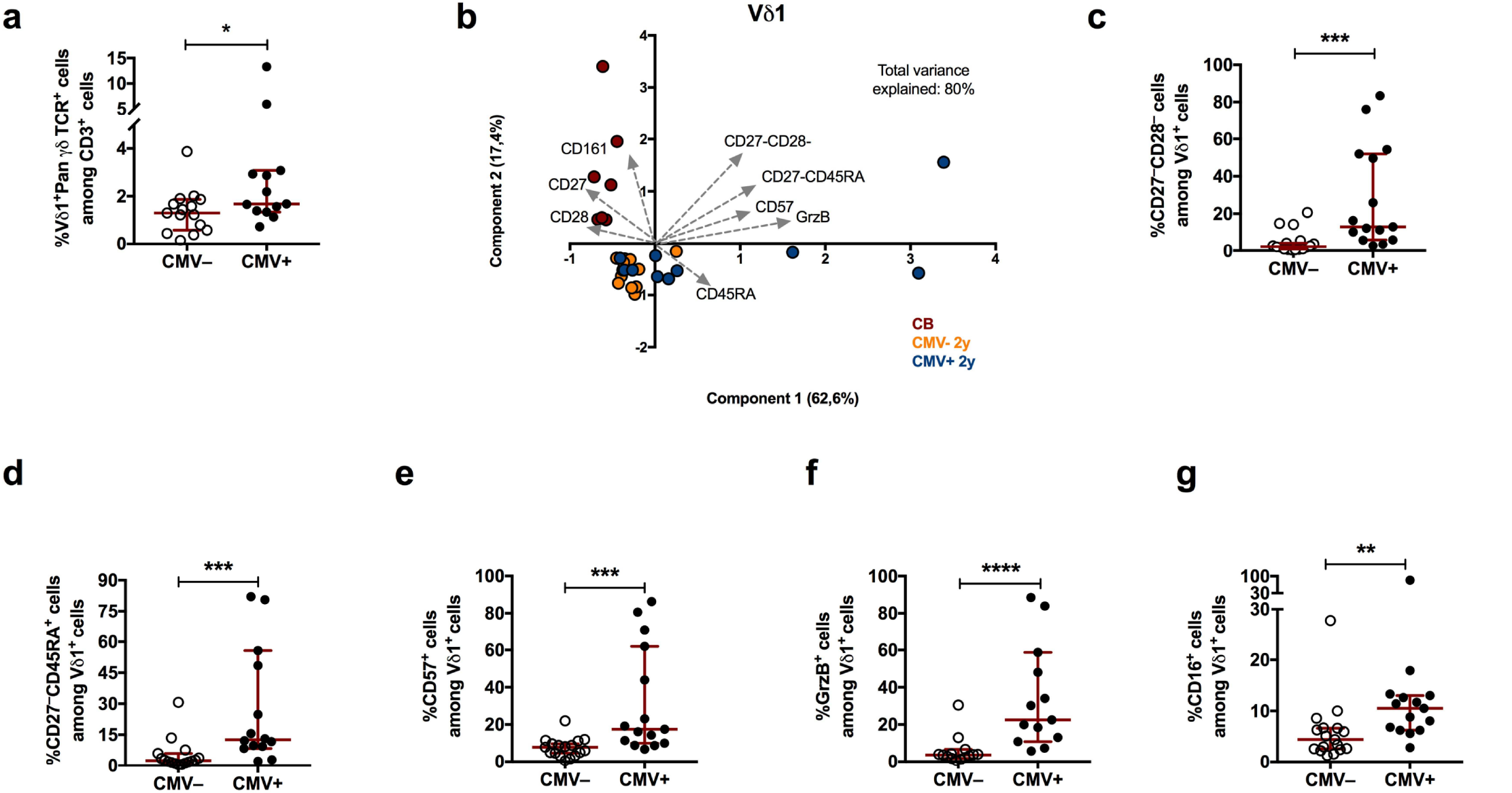
a
*
%Vδ1+Pan γδ TCR+ cells among CD3+ cells
15
10
5
4
2
0
CMV–
CMV+
b
Vδ1
Total variance explained: 80%
Component 2 (17,4%)
CD161
CD27
CD28
CD27-CD28-
CD27-CD45RA
CD57
GrzB
CD45RA
CB
CMV- 2y
CMV+ 2y
Component 1 (62,6%)
c
***
%CD27−CD28− cells among Vδ1+ cells
100
80
60
40
20
0
CMV–
CMV+
d
***
%CD27−CD45RA+ cells among Vδ1+ cells
90
75
60
45
30
15
0
CMV–
CMV+
e
***
%CD57+ cells among Vδ1+ cells
100
80
60
40
20
0
CMV–
CMV+
f
****
%GrzB+ cells among Vδ1+ cells
100
80
60
40
20
0
CMV–
CMV+
g
**
%CD16+ cells among Vδ1+ cells
100
30
30
20
10
0
CMV–
CMV+